ACS OMEGA

http://pubs.acs.org/journal/acsodf

Article

# Experimental Study on Catalytic Action of Intrinsic Metals in Coal Spontaneous Combustion

Ling Qiao, Xiaogang Mu, Cunbao Deng, Xuefeng Wang, and Yansheng Wang*

Cite This: *ACS Omega* 2023, 8, 13680−13689

Read Online

ACCESS | Metrics & More | Article Recommendations

**ABSTRACT:** In order to study the effect of inherent metals in coal on spontaneous combustion, Hongmiao lignite and Hongqingliang long-flame coal were demineralized by hydrochloric acid, the raw coal and demineralized coal were characterized by Fourier transform infrared spectrometry, X-ray diffraction, and synchronous thermal analysis experiments, and the corresponding ash content was detected by inductively coupled plasma mass spectrometry. The results show that the effect of demineralization on the volatile matter of low-rank coal is small, and the change of crystallite structure is not significant. The removed parts are mainly water-soluble salts and soluble minerals, such as carbonates and metal ions, that are not tightly bound to the organic matter of coal structure. The removed metal elements are mainly alkali metals Na and K, alkaline earth metals Ca, Mg, Sr, and Ba, and transition metals Fe, Mn, Ti, and so forth. The temperatures corresponding to the end of weight loss, ignition, and maximum weight loss rates were elevated on the thermogravimetric curves of the demineralized coal samples. The heat absorbed by evaporation of water in coal and the heat released by oxidation and combustion of coal are decreased to different degrees, indicating that the spontaneous combustion tendency of coal after demineralization is reduced, and alkali metal, alkaline earth metals, and transition metals in coal have a catalytic effect on spontaneous combustion of coal. After adding the metal chelating agent ethylenediaminetetraacetic acid (EDTA), the apparent activation energy decreased by 33.08 and 2.42%, respectively. EDTA and the alkali metal, alkaline earth metal, or transition-metal ions formed a stable chelate in coal. The catalytic activity of metals is weakened or even lost, thereby inhibiting spontaneous combustion of coal, and verifying the catalytic effect of internal metals in coal on the spontaneous combustion of coal.

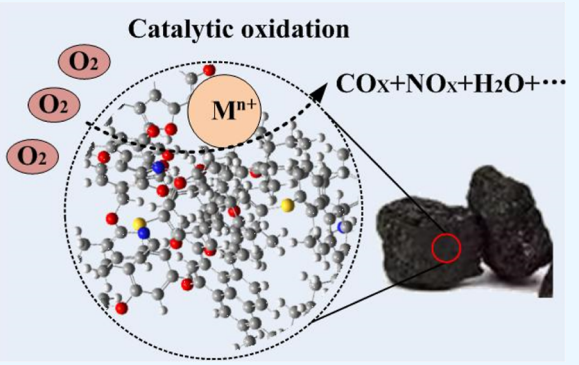


## 1. INTRODUCTION

Coal spontaneous combustion is one of the most serious mine disasters, which brings serious hidden dangers to the safe production and transportation of coal, as well as waste resources and polluting environment.[1,2] The reason for coal spontaneous combustion is currently recognized as the theory of coal−oxygen compounding. The coal reacts with the oxygen in the air to produce heat, which causes coal spontaneous combustion. Research on the mechanism of spontaneous combustion of coal has focused on the reaction between organic matter in coal and oxygen, and the inhibition of spontaneous combustion of coal has been achieved by inhibiting the reaction between organic matter in coal and oxygen.

Coal is a complex mixture of organic matter and inorganic minerals, with inorganic minerals accounting for between 1 and 30%.[3] Affected by the geological conditions during the coal-forming period, the mineral composition of different coals is diverse, and the types and contents of metal elements are also quite different. At present, 64 kinds of metal elements have been found in Chinese coal.[4] In catalytic science, metals and their compounds are widely used as catalysts. Metals, such as Na, K, Ca, Mg, Mn, Zn, Fe, and Ni, are considered to have catalytic activity for coal pyrolysis and gasification.[5−10] Transition metals, such as Fe and Ni, and minerals, such as montmorillonite, have been shown to have a catalytic effect on organic matter.[11−14] The presence of inorganic matter can advance the peak of gas generation from organic matter in coal seams. The aim of the above research is to find a suitable catalyst to improve the yield of the product. In the process of pulverized coal combustion, alkali metals, alkaline earth metals, and transition metals, such as Fe, Mn, Cu, Zn, and Ce, are added as catalysts to improve the coal combustion efficiency.[15−20] Different from the reactivity of the combustion reaction after the high-temperature section, that is, after the ignition point, it is studied that the spontaneous combustion of

Received: December 5, 2022
Accepted: March 27, 2023
Published: April 7, 2023

coal pays more attention to the oxidation reaction of coal before the ignition point. The temperature has an important influence on the chemical reaction rate and diffusion process.[21,22] In different temperature ranges, the control mechanism of the reaction is different. In addition, temperatures have a great influence on the activity of the catalyst, and there is a great difference between pulverized coal combustion and coal spontaneous combustion.

There is clear evidence that the added metal compounds have changed the spontaneous combustion properties of the coal. Tang[23] proved that manganese-containing additives can promote coal spontaneous combustion through experiments, and it is believed that $Mn^{2+}$ enhances the formation of free radicals in coal by strengthening transfer electrons. Larionov et al.[24] experimentally proved that $Na^+$ and $Cu^{2+}$ can reduce the initial oxidation temperature of coal and promote the spontaneous combustion process of coal. Zhang and Sujanti[25] experimentally studied that the addition of $Mg(Ac)_2$, $CaCl_2$, and NaCl inhibited the low-temperature oxidation of coal, while $Cu(Ac)_2$, KAc, and NaAc promoted the low-temperature oxidation. Lv et al.[26] analyzed the ignition risk of coal spontaneous combustion under the influence of NaCl, KCl, and $MgCl_2$ solutions using hot plate tests, the results showed that NaCl and KCl promoted coal spontaneous combustion, while the $MgCl_2$ solution inhibited it. Qiao et al.[27] investigated calcium catalysis of coal spontaneous combustion and showed that calcium oxide largely promoted coal spontaneous combustion, while calcium carbonate and calcium acetate promoted it slightly. Lu et al.[28] investigated the effect of pyrite oxidation products on coal spontaneous combustion and showed that $Fe^{3+}$ and $Fe^{2+}$ promoted the development of C═O and −CO−O− and accelerated the oxidation of $-CH_3$, $-CH_2-$, and −OH to promote the low-temperature oxidation of coal. Liu et al.[29] found that sulfate-rich mine water ($Ca^{2+}$ and $Mg^{2+}$) inhibited the formation of −OH and accelerated the cracking of aromatic rings in the process of coal oxidation, which can effectively inhibit the combustion of coal. The reason for these differences may be that the added compounds and the intrinsic metals in the coal are different in their form and distribution.

There are three main types of intrinsic metal elements in coal:[30,31] water-soluble state, metal ions dissolved in pore water; organically bound state: metal elements in the form of H or oxygen-containing functional groups in coal by adsorption, ion exchange, or coordination; and discrete mineral matters. Some scholars have separated inorganic minerals from organic matter by inorganic acid washing, such as nitric acid,[32] sulfuric acid,[33] hydrofluoric acid,[34,35] hydrochloric acid,[36] or combined acid pickling,[37−40] and analyzed the effect of demineralization on coal structures. Studies have shown that the addition of nitric acid tends to cause oxidation and nitrification of coal, and the introduction of nitro groups causes a large change in the coal structure and morphology.[41] The addition of sulfuric acid causes a sulfonation reaction to introduce a sulfonic acid group into the coal structure.[42] HF has a greater impact on coal volatiles,[41] especially for low-rank coal, and the change in volatiles will inevitably lead to changes in the spontaneous combustion characteristics of coal, making the coal sample lose comparability with the original coal sample after elution. Although the above pickling method can reduce the ash to a very low level, it has a great influence on the organic structure of coal, which affects the accuracy of the subsequent experimental analysis results. Song et al.[34] only used hydrochloric acid to treat the Shengli lignite, removing 55% of the minerals, and its surface morphology and organic structure are still ideal.

Zhou et al.[42] found that the main part of the catalytic activity was minerals that could be dissolved in hydrochloric acid eluents. The main components of insoluble minerals are silicate and aluminosilicate. Studies show that aluminum may play a negative catalytic role.[34] In the low-rank coal, the content of active metal components is relatively high. With the deepening of the degree of metamorphism, these metal elements gradually transform from water-soluble and organically bound states into insoluble salts, and it is speculated that the activity of metal elements in low-rank coal is higher.

In view of this, two low-rank coals with different metamorphic degrees are used in this experiment, Hongmiao lignite and Hongqingliang long-flame coal. The effect of intrinsic metal in coal on the spontaneous combustion characteristics of coal is studied by using hydrochloric acid demineralization. The metal elements with catalytic activity were found out, and the appropriate metal chelating agent was selected as the inhibitor to verify the catalytic effect of metals in coal on the spontaneous combustion of coal. It provides new ideas and methods for mine fire prevention.

## 2. EXPERIMENTS AND METHODS

**2.1. Sample Preparation.** Hongmiao (HM) lignite and Hongqingliang (HQL) long-flame coal samples were used as experimental coal samples. After collecting the coal samples, they were sealed immediately and brought to the laboratory. Coal samples were crushed and screened. 100−250 mesh coal samples were selected and sealed in clean and dry wide-mouth bottles. Labels were affixed to indicate sampling time and location for reserve.

The two coal samples were added with 18% HCl in a ratio of 1 g:5 mL and heated in a water bath at 60 °C with constant stirring for 2 h. The solution was filtered and washed until it was neutral. After that, the samples were dried in a vacuum drying oven at 60 °C for 4 h. They were recorded as HM-D and HQL-D, respectively. The proximate analysis of coal samples was measured according to Chinese standard GB/T212-2008, and the results are shown in Table 1.

**Table 1. Proximate Analysis of Coal Samples**

| code | $M_{ad}$/% | $V_{ad}$/% | $FC_{ad}$/% | $A_{ad}$/% | $S_{t,d}$/% |
|---|---|---|---|---|---|
| HM | 9.60 | 30.09 | 51.95 | 8.36 | 0.98 |
| HM-D | 8.48 | 31.56 | 54.67 | 5.29 | 0.88 |
| HQL | 8.50 | 29.46 | 55.65 | 5.39 | 0.26 |
| HQL-D | 8.51 | 29.94 | 59.26 | 2.29 | 0.25 |

The two raw coals were wetted with a small amount of acetone, then added into an ethylenediaminetetraacetic acid (EDTA) thermal saturated solution in a ratio of 1 g:4 mL, sealed and stationary for 1 week, and dried in a vacuum drying box at 60 °C for 4 h, which were designated as HM-E and HQL-E.

**2.2. Experimental Procedures.** *2.2.1. Ash Composition Detection.* According to the slow ashing method, four kinds of coal samples were ashed in a muffle furnace. After being digested by a microwave digestion instrument, Agilent inductively coupled plasma mass spectrometry (ICP−MS) 8800 was used to detect the main metal components in raw



https://doi.org/10.1021/acsomega.2c07741
ACS Omega 2023, 8, 13680−13689

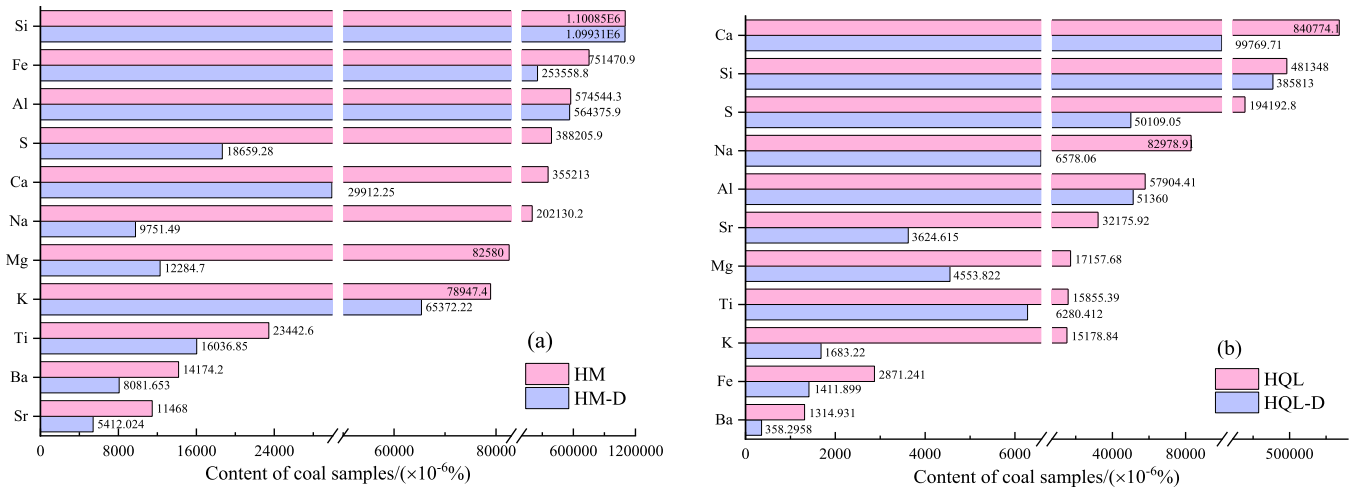


**Figure 1.** Distribution of metal composition in coal: (a) HM and HM-D and (b) HQL and HQL-D.

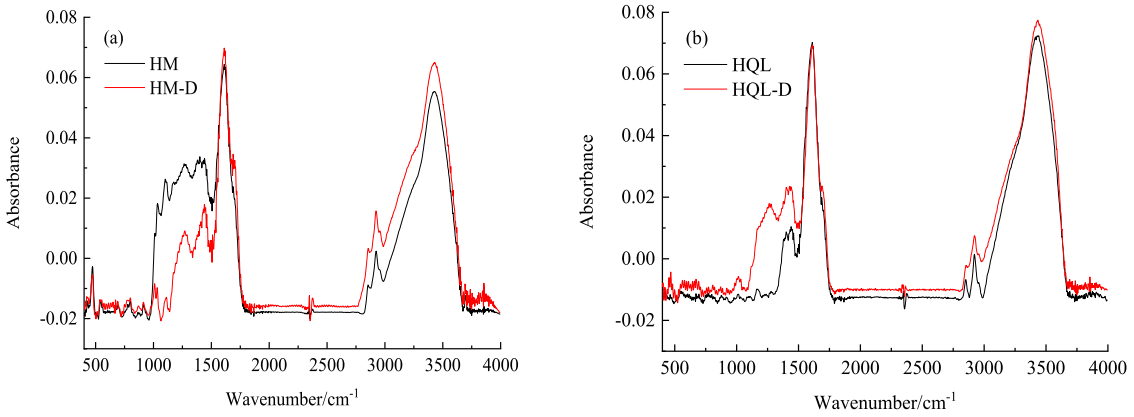


**Figure 2.** FT-IR of coal samples: (a) HM and HM-D and (b) HQL and HQL-D.

coal and corresponding demineralized coal. The parameters are set as follows. RF power: 15,500 W; plasma gas flow rate: 18 L/min; carrier gas flow rate: 1.2 L/min; auxiliary gas flow rate: 0.9 L/min; nebulizer chamber temperature: 2 °C; nebulizer: concentric nebulizer; sampling cone, and intercept cone are nickel cone; and sampling depth: 8 mm.

*2.2.2. Fourier Transform Infrared Spectrometer of Coal Samples.* A TENSOR27 Fourier transform infrared spectrometry (FT-IR) was used. The coal samples was ground to a particle size of less than 250 mesh using an agate mortar, dried at a constant temperature of 110 °C, uniformly mixed with a spectrally pure KBr at a ratio of 1:180, and then ground and compressed. The pressed samples were put into the instrument and scanned 32 times, and infrared spectra of the tested samples were obtained.

*2.2.3. X-ray Diffraction.* The X-ray diffraction (XRD) spectra were acquired on a D8 ADVANCE X-ray diffractometer manufactured by Bruker, Germany. The coal sample was ground to below 250 mesh and loaded on an aluminum frame holder. The experiment used copper target radiation, ceramic X-ray tube, tube voltage 40 kV, tube current 35 mA, with scanning speed 2°/mm, and scanning range 5−90°.

*2.2.4. Synchronous Thermal Analysis Experiment.* The experimental equipment used was a STA449C comprehensive thermogravimetric (TG) analyzer from NETZSCH. Experimental conditions: the quality of samples is about 15 mg, heating rate of 5 °C/min, flow velocity of oxygen and nitrogen were 10 and 40 mL/min, simulated air component ratio, and testing temperature range is set to 25−800 °C.

## 3. RESULTS AND DISCUSSION

**3.1. Component Analysis of Coal Ash.** From the calculation in Table 1, the volatile matter of the HM coal sample and HQL coal sample treated with hydrochloric acid has little change in the volatile matter. The ash removal rates of coal sample reaches 36.72 and 57.51%, respectively, which indicates that hydrochloric acid treatment can effectively remove minerals from low-rank coal.

According to ICP−MS measurement results, the elements content in coal ash is converted into the percentage of element content in coal, and the metal elements with higher content in the coal sample are shown in Figure 1.

The metal elements in coal seams are derived from those contained in coal-forming plants and those that entered the coal seams during the geological transformation of coal and are related to paleontological and geochemical characteristics to the depositional environment, depositional history, and climate and plant changes. The types and contents of metal elements in the two coal samples in Figure 1 are quite different, which is related to the geological conditions of the coal-forming period. Both coal samples are similar in that they have higher Al content and the effect of hydrochloric acid treatment on Al content is less because most of the Al elements exist in the form of silicoaluminates, which are stable and insoluble in



https://doi.org/10.1021/acsomega.2c07741
ACS Omega 2023, 8, 13680−13689

hydrochloric acid. The summed removal rates of Si and Al were 2.0% for HM and 18.8 for HQL.

Figure 1a shows that Fe, Ca, Na, and Mg are the elements with high content and high removal rate in the HM coal sample. The removal rates after hydrochloric acid treatment are 66.3, 91.6, 95.2, and 85.1%, respectively. Figure 1b shows that Ca, Na, and Sr are the most abundant elements in the HQL coal sample, and the removal rates after hydrochloric acid treatment are 88.1, 92.1, and 88.8%, respectively. The contents of Ti and Mn in transition metals except Fe are relatively high in the two coal samples. The removal rates of Ti and Mn in the HM coal sample are 33.0 and 98.4%, while those in HQL are 60.4 and 83.1%.

Soluble minerals, such as water-soluble organic-bound carbonate, can be removed from coal by hydrochloric acid treatment. The removed metal elements are mainly alkali metals Na and K, alkaline earth metals Ca, Mg, Sr, and Ba, and transition metals Fe, Mn, Ti, and so forth. The insoluble salts such as silicate and aluminosilicate were not removed.

**3.2. FT-IR Analysis.** The infrared spectra of coal samples are shown in Figure 2. According to previous studies,[43−47] the attribution of absorption peaks is shown in Table 2.

**Table 2. FT-IR Absorption Peak Attribution of Functional Groups**

| number | peak/cm$^{-1}$ | functional group |
|---|---|---|
| 1 | 700−900 | substituted benzene |
| 2 | 1000 | the minerals |
| 3 | 1110−1330 | Ar−CO |
| 4 | 1380 | bending vibration absorption peak of $-CH_3$ |
| 5 | 1430 | out-of-plane bending vibration of $-CH_2-$ |
| 6 | 1600 | the stretching vibration of aromatic ring C=C |
| 7 | 1628 | the aromatic nuclear vibration of phenolic hydroxyl group |
| 8 | 1716 | carboxyl group |
| 9 | 2850 | symmetrical stretching vibration of $-CH_2-$ |
| 10 | 2920 | $-CH_2-$ antisymmetric stretching vibration |
| 11 | 3030 | aromatics absorption peak of −CH−, which is related to the absorption at 870, 820, and 750 cm$^{-1}$ |
| 12 | 3400 | the vibration absorption peak of −OH stretching |

Some changes have taken place in the structure of HM coal sample after treatment with hydrochloric acid. The absorption peaks of minerals near 1000 cm$^{-1}$ were weakened. The vibration of alkyl ethers and aryl ethers near 1100 cm$^{-1}$ was strengthened. The flexural vibration of $-CH_3$ and $-CH_2-$ at 1375 and 1430 cm$^{-1}$ was strengthened, which indicates the increase of the fat hydrocarbon structure in coal. The stretching vibration absorption peaks of aromatic ring C=C at 1500 cm$^{-1}$ did not change significantly, indicating that hydrochloric acid treatment did not affect the benzene ring skeleton structure of coal molecules. The stretching vibration of carboxylic group at 1700 cm$^{-1}$ is obviously enhanced because carboxylate loses metal ions and converts to covalent carboxylic acid under the action of hydrochloric acid.[48] The broadening of the vibration absorption peak of −OH at 3400 cm$^{-1}$ indicates that the cross-linking of hydrogen bonds in the coal macromolecular structure is enhanced.

After the demineralization of the HQL coal sample, the absorption peaks of minerals near 1000 cm$^{-1}$ were obviously weakened. The absorption peaks of alkyl ether and aryl ether C=C stretching vibration and $-CH_2-$ and $-CH_3$ absorption peaks did not change significantly. The C−O stretching vibration of the phenolic hydroxyl group at 1250 cm$^{-1}$ was enhanced. The stretching vibration of aromatic ring C=C at 1500 cm$^{-1}$ did not change significantly, indicating that demineralization had a slight effect on the benzene ring skeleton domain of HQL coal samples. The stretching vibration of the carboxyl group at 1700 cm$^{-1}$ was slightly enhanced, indicating that the carboxylate loses metal ions and converts to covalent carboxylic acid. At 3400 cm$^{-1}$, there was no obvious change in the absorption peak of −OH stretching vibration.

The main changes in IR spectra of the coal samples are reflected in two aspects, one is the obvious weakening of the mineral peaks around 1000 cm$^{-1}$, caused by the removal of minerals. Combined with the analysis of coal ash composition, it can be considered as the removal of soluble minerals, such as water-soluble salts and carbonates. The second is the enhancement of the carboxyl absorption peak at 1700 cm$^{-1}$ because the carboxylate is generated by the action of $H^+$.

The effect of demineralization on the coal structure mainly includes two parts: first, the removal of inorganic minerals, including soluble minerals, such as water-soluble salts and carbonates and second, the removal of metals with organic binding states, which are not tightly bound to oxygen-containing functional groups, so that organic salts become organic acids, such as carboxylates generate carboxylic acids under the action of $H^+$, leading to the change of coal structure.

**3.3. Microcrystalline Structure of Coal.** As can be seen from Figure 3, there are two distinct diffraction peaks, 002 and 100 peaks in the experimental coal samples. The $2\theta$ angles of the 002 peaks are all around 24°, and the degree of graphitization is low. In theory, the 002 peak is symmetrical, which is generated by the superposition of 002 band and $\gamma$ band. The asymmetry is due to the vibration of $\gamma$ band on its left side. Peak fitting was used to fit 002, $\gamma$, and 100 peaks. According to the half-peak width and diffraction angle of X-ray diffraction patterns, the parameters of coal microcrystalline structure are calculated by the Bragg equation and Schrer equation.[49,50]

$$d_{002} = \lambda/(2\ \sin\theta_{002}) \quad (1)$$

$$d_{100} = \lambda/(2\ \sin\theta_{100}) \quad (2)$$

$$L_c = 0.94\lambda/(\beta_{002}\ \cos\theta_{002}) \quad (3)$$

$$L_a = 1.84\lambda/(\beta_{100}\ \cos\theta_{100}) \quad (4)$$

$$M_c = L_c/d_{002} \quad (5)$$

$\lambda$ is the X-ray wavelength with a value of 0.154 nm, $d_{002}$ and $d_{100}$ are the distances of the laminar layer, nm, $\theta_{002}$ and $\theta_{100}$ are Bragg angles corresponding to the peaks 002 and 100, $\beta_{002}$ and $\beta_{100}$ are the half peak width corresponding to 100, $L_c$ is the stacking height of the laminar layer, nm, $L_a$ is the diameter of the laminar layer, nm, $M_c$ is the number of effective stacking of the laminar layer, and $f_a$ is the aromaticity of coal samples. According to formula 6, the aromaticity of coal samples can be calculated

$$f_a = C_{ar}/(C_{ar} + C_{al}) = A_{002}/(A_{002} + A_\gamma) \quad (6)$$

The results are shown in Table 3.

There is no significant change in the aromaticity of the coal sample after demineralization. The distance between aromatic



https://doi.org/10.1021/acsomega.2c07741
ACS Omega 2023, 8, 13680−13689

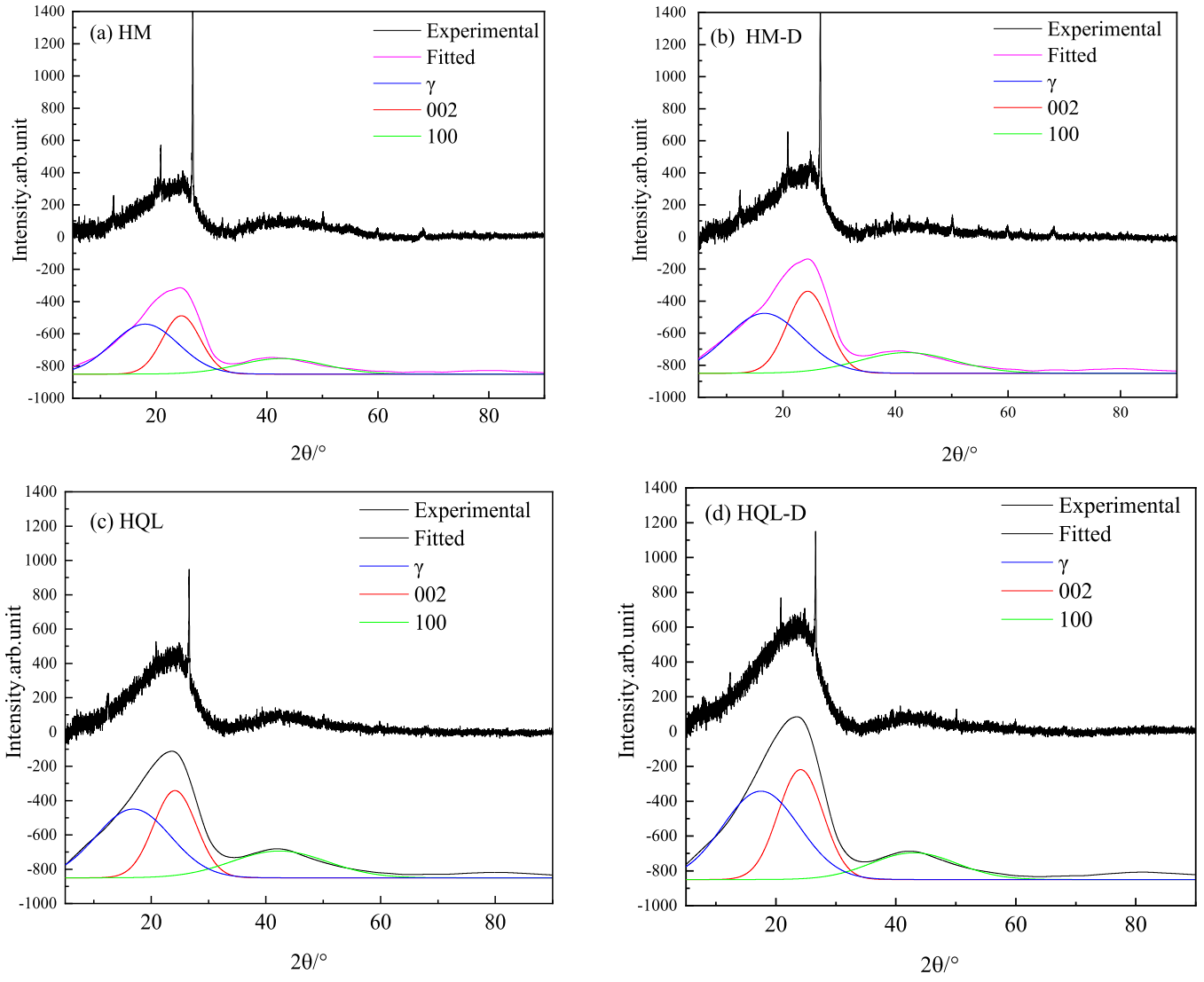


**Figure 3.** XRD of coal samples: (a) HM, (b) HM-D, (c) HQL, and (d) HQL-D.

**Table 3. Microcrystalline Structure Parameters of Coal Samples**

| code | $d_{002}$ | $L_c$ | $d_{100}$ | $L_a$ | $M_c$ | $f_a$ |
|---|---|---|---|---|---|---|
| HM | 0.362 | 1.059 | 0.212 | 0.966 | 2.927 | 0.400 |
| HM-D | 0.364 | 0.991 | 0.215 | 0.869 | 2.720 | 0.420 |
| HQL | 0.368 | 0.968 | 0.213 | 0.888 | 2.630 | 0.421 |
| HQL-D | 0.369 | 0.962 | 0.212 | 1.039 | 2.610 | 0.429 |

layers of the two kinds of coal samples remained basically unchanged. The stacking height, diameter of aromatic layers, and the number of effective aromatic layers of coal samples of HM decreased. The diameter of aromatic layers of coal samples of HQL increased slightly, while the stacking height and the number of effective aromatic layers remained basically unchanged. This indicates that hydrochloric acid treatment has no significant effect on the microcrystalline structure of low-order coal and has a weaker effect on long-flame coal.

**3.4. Characteristic Temperature Analysis.** TG curves record the relationship between sample quality and temperature or time. The first-order differential curve of TG is recorded as derivative TG (DTG), which is used to characterize the change of sample quality. The TG−DTG curve of the experimental coal sample is shown in Figure 4. The ignition point of coal is defined as the intersection point of the straight line parallel to the *Y* axis and the tangent line of the maximal weight-losing rate temperature on the TG curve.

According to the trend of the curve, the oxidation and spontaneous combustion process of coal samples can be divided into three stages: dehydration, oxidation, and combustion.

In the dehydration stage, free water evaporates from coal, accompanied by the precipitation of a small amount of adsorbed primary gas, such as $CO_2$, $N_2$, and $CH_4$, and volatilization of volatile matter, and the mass of coal sample decreases, showing the weight loss on the TG curve.

During the oxidation stage, the range is from the end point of weightlessness to the ignition point of coal sample, during which the coal after drying begins to absorb oxygen, bridging bonds, side-chain groups, oxygen functional groups, and some small molecules undergo oxidation reaction in the molecular structure of coal. The adsorption capacity of coal to oxygen is enhanced. When the adsorption capacity is greater than the mass of escaping gas, it shows the weight gain on the TG curve; on the contrary, it decreases.


https://doi.org/10.1021/acsomega.2c07741
ACS Omega 2023, 8, 13680−13689

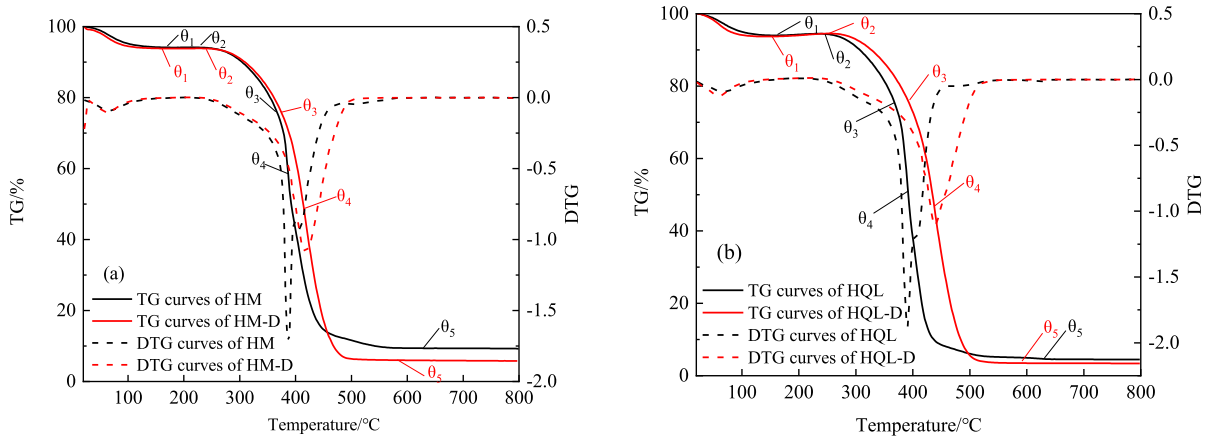


**Figure 4.** TG−DTG curves of coal samples: (a) HM and HM-D and (b) HQL and HQL-D.

**Table 4. Characteristic Temperature of Coal Samples/°C**

| code | temperature of dehydration end point $\theta_1$ | temperature of weight gain end point $\theta_2$ | ignition temperature $\theta_3$ | temperature of maximum weight loss rate $\theta_4$ | burnout temperature $\theta_5$ |
|---|---|---|---|---|---|
| HM | 184.1 | 216.8 | 366.5 | 386.8 | 624.8 |
| HM-D | 172.6 | 229.3 | 374.0 | 416.3 | 572.3 |
| HQL | 160.4 | 245.8 | 368.4 | 390.0 | 635.7 |
| HQL-D | 145.8 | 252.3 | 393.1 | 438.3 | 596.4 |

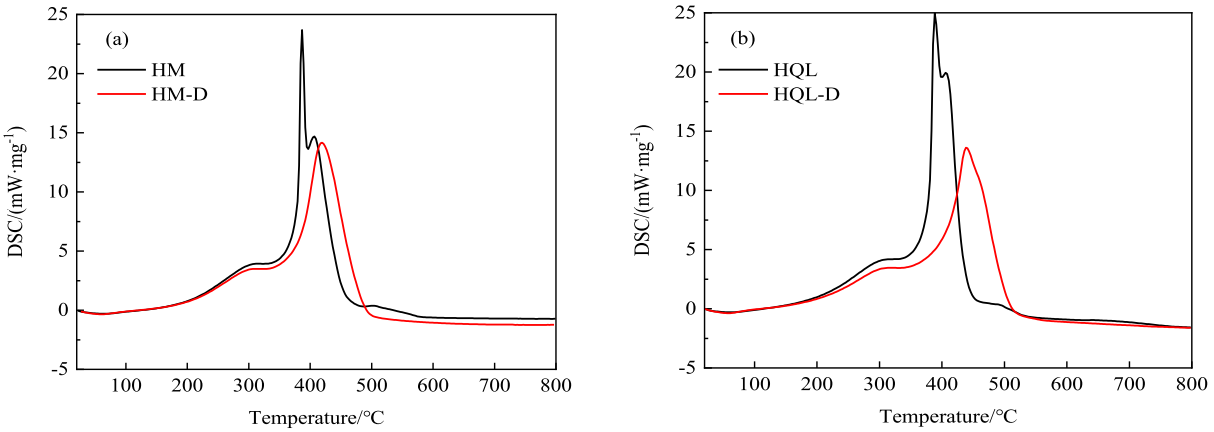


**Figure 5.** DSC curves of coal samples: (a) HM and HM-D and (b) HQL and HQL-D.

The combustion stage is the temperature from the ignition point to mass reduced to constant weight of the coal sample. In this stage, the coal burns violently, producing a large number of gas products, and the mass decreases sharply. At the temperature of the maximum weight loss rate, the molecular skeleton structure of coal is broken. When the mass of coal decreases to constant, the coal burns out.

Characteristic temperature of coal samples is shown in Table 4.

The dehydration stage is a process in which water changes into the gasification phase and separates from coal under continuous heating. As shown in Table 4, the temperatures at the end of dehydration of the demineralized coal sample were 11.5 and 14.6 °C lower than that of the raw coal, indicating that metal ions have an inhibiting effect on water evaporation. Water molecules adsorbed at carboxylate on the surface of coal form metal-ion water cluster $I^+(H_2O)_n$ with metal ions.[51,52] With the increase of metal ions, the adsorption of water molecules is enhanced. The conversion of carboxylate into carboxylic acid in demineralized coal decreases the adsorption capacity of water, accelerates the process of water loss, and advances the temperature of water loss.

The temperature of the end of the weight gain, the ignition temperature and the maximal weight-losing rate temperature of HM-D were increased by 6.1, 7.5, and 29.5 °C, respectively, compared with HM. The same phenomenon occurred in HQL-D, and the temperature of the three characteristic points was increased by 6.5, 24.7, and 48.3 °C compared with HQL. It shows that the spontaneous combustion tendency of demineralized coal is reduced. This is because, on the one hand, metal ions have a catalytic effect on the oxidation reaction of coal and , on the other hand, the metal surface provides more active centers for coal molecules to react with oxygen, which is conducive to coal oxidation. Therefore, demineralization inhibits the oxidation and combustion of coal.

The demineralized coal reaches the burnout temperature ahead of time because part of the organic matter in raw coal is wrapped in minerals and burns after 500 °C. Most of the minerals in the demineralized coal are removed, and the


https://doi.org/10.1021/acsomega.2c07741
ACS Omega 2023, 8, 13680−13689

Table 5. Parameters of Heat Change of Experimental Coal

| | water evaporating endothermic peak | | | oxidation exothermic peak | | | combustion exothermic peak | | |
|---|---|---|---|---|---|---|---|---|---|
| code | range | peak value/°C | heat quantity/J·g$^{-1}$ | range | peak value/°C | heat quantity/J·g$^{-1}$ | range | peak value/°C | heat quantity/J·g$^{-1}$ |
| HM | 25.0−146.2 | 74.5 | −456.9 | 146.2 | 293.3−330.4 | 434.3 | 330.4−598.5 | 386.9 | 10054 |
| HM-D | 25.0−150.3 | 66.1 | −418.5 | 150.3 | 294.3−332.6 | 414.9 | 332.6−576.3 | 420.6 | 9801 |
| HQL | 25.0−135.6 | 74.9 | −571.9 | 135.6 | 283.7−350.4 | 384.0 | 350.4−550.0 | 388.5 | 9705 |
| HQL-D | 25.0−132.2 | 61.3 | −523.3 | 132.2 | 298.0−356.7 | 314.5 | 356.7−578.3 | 439 | 9489 |

organic matter is exposed to the air and burns completely in advance.

**3.5. Thermal Change Analysis.** Differential scanning calorimetry (DSC) curves record the variation of energy difference with time between the sample and the reference material. The DSC curves of the coal samples are shown in Figure 5. The DSC curve shows a small heat absorption peak at 60−70 °C, which is mainly caused by the evaporation and heat absorption of water in coal. In the low-temperature oxidation stage of coal, the heat absorbed by water evaporation is much higher than the wetting heat of water to coal, and the area of this endothermic peak mainly depends on the moisture content of coal. A slow exothermic peak occurs near 290 °C, which is the heat released by the rapid physical−chemical reaction between dry coal and oxygen. There is a large exothermic peak at 387−439 °C, which is the heat released from coal combustion.

As shown in Figure 5, HM and HQL have changed obviously after hydrochloric acid treatment. The maximum exothermic peak of HM occurs at 386.9 °C, the maximum heat flux reaches 23.69 mW/mg, while the maximum heat flux peak occurs at 420.6 °C for demineralized coal, and the maximum heat flux is 14.17 mW/mg. A similar change trend of HQL coal samples after demineralization was also observed. The maximum exothermic peak was increased from 388.5 to 439 °C, and the maximum heat flux was reduced from 24.95 to 13.59 mW/mg. It shows that the oxidation exothermic rate of demineralized coal is low, and the extreme point of heat flow is increased. After 410 °C, the reaction rate is controlled by the residual amount of reactants. In addition, metal/minerals cover the surface of coal, resulting in the plugging effect. The heat flow rate of raw coal is lower than that of demineralized coal.

The heat change in the reaction process can be calculated by integrating the DCS curve. The heat variation parameters of the experimental coal samples are shown in Table 5. As it is shown, the heat absorption of water evaporation of HM is 456.9 J/g and the ash removal coal is 418.5 J/g, reduced by 8.3%. After hydrochloric acid treatment, the heat released by water evaporation of HQL decreased from 571.9 to 523.3 J/g, which decreased by 8.5%. The ability of demineralized coal to absorb water was reduced, and the rate of water loss was faster, which led to the decrease of heat absorbed by water evaporation.

The oxidative heat release of HM is 434.3 J/g, which decreases to 414.9 J/g after demineralization, and decreases by 4.5%. The oxidation heat of HQL is 384.0 J/g, which decreases to 314.5 J/g after demineralization, and decreases by 22.1%. The oxidative heat release of experimental coal samples after demineralization is lower than that of raw coal. From the point of view of heat change, the spontaneous combustion tendency of demineralized coal decreases, indicating that inherent metals in low-rank coal play a stimulative role in the process of spontaneous combustion for coal.

The combustion heat of HM is 10,054 J/g, which decreases to 9801 J/g after demineralization, and decreases by 2.5%. The combustion heat release of HM is 9705 J/g, which decreases to 9489 J/g after demineralization, and decreases by 2.2%. The combustion heat release decreases and the combustion performance of demineralized coal decreases, indicating that inherent metals in low-rank coal also promotes the coal combustion process.

**3.6. Inhibitory Effect of Metal Chelating Agent on Spontaneous Combustion of Coal.** EDTA has a wide range of coordination properties. It can form stable chelates with alkaline earth metals and most transition-metal ions, and the stability constants of the chelates formed are very large. Its chemical structure is shown as Figure 6.

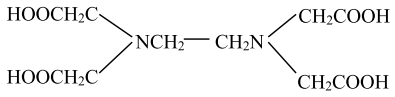


Figure 6. Chemical structure of EDTA.

It has six ligands, four carboxyl oxygen and two amino nitrogen can be used as ligands for the teeth, which coordinate with metal ions to form a chelate with high five-membered ring stability, which reduces metal ions or loss of reactivity. EDTA has different complexing abilities to different metal elements, as shown in Table 6, and when the content of these elements in a certain coal is high, the inhibitory effect is obvious. Therefore, EDTA was selected as an inhibitor to verify the catalytic effect of metals on coal spontaneous combustion.

The TG−DTG curves of experimental coal samples are shown in Figure 7. It can be seen that the mass of HM and HQL increased slightly on the TG curve after the dehydration stage, because the mass of oxygen adsorbed by coal oxidation is greater than the mass of volatile gas. However, after adding EDTA, the quality of the two samples kept decreasing, resulting in no point $\theta_2$. It shows that the oxygen absorbed by coal is less than the volatile gas when it just enters the oxidation stage. It shows that EDTA inhibits the adsorption of oxygen on coal samples at the low-temperature stage. The characteristic temperatures of the coal samples are shown in Table 7. The ignition temperatures of the two coal samples increased by 11.7 and 7 °C, respectively. Moreover, the maximal weight-losing rate temperature of HM is increased by 40.5 °C and that of HQL is increased by 25.0 °C.

According to the Arrhenius formula, using the data of conversion in the range of 15−90% on TG curves, the reaction between coal and oxygen is a first-order reaction. The reaction model is set as $f(x) = (1 - x)$, where $x$ is the conversion of the reaction.

$$dx/dt = A \exp(-E/RT)(1 - x) \quad (7)$$



https://doi.org/10.1021/acsomega.2c07741
ACS Omega 2023, 8, 13680−13689

**Table 6. Coordination Constants of EDTA and Metal Ions**

| $Na^{+}$ | $Ca^{2+}$ | $Ba^{2+}$ | $Sr^{2+}$ | $Mg^{2+}$ | $Fe^{3+}$ | $Al^{3+}$ | $Zn^{2+}$ | $Cu^{2+}$ | $Ti^{3+}$ |
|---|---|---|---|---|---|---|---|---|---|
| 1.7 | 10.7 | 7.9 | 8.7 | 8.7 | 14.3 | 16.1 | 16.5 | 18.8 | 21.3 |

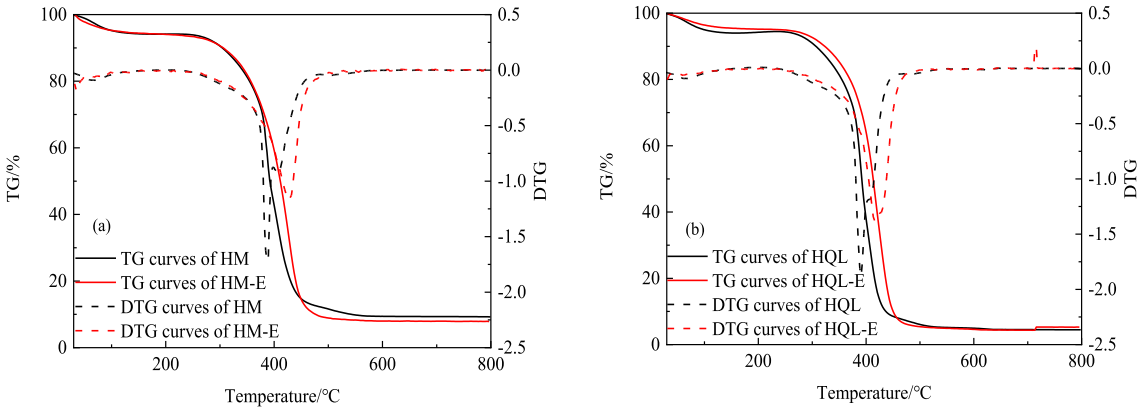


**Figure 7.** TG−DTG curves of coal samples: (a) HM and HM-D and (b) HQL and HQL-D.

**Table 7. Characteristic Temperature of Coal Samples/°C**

| code | temperature of dehydration end point $\theta_1$ | temperature of weight gain end point $\theta_2$ | ignition temperature $\theta_3$ | temperature of maximum weight loss rate $\theta_4$ | burnout temperature $\theta_5$ |
|---|---|---|---|---|---|
| HM | 184.1 | 216.8 | 366.5 | 386.8 | 624.8 |
| HM-E | 162.3 | | 378.2 | 427.3 | 618.3 |
| HQL | 160.4 | 245.8 | 368.4 | 390.0 | 635.7 |
| HQL-E | 163.3 | | 375.4 | 415.0 | 625.4 |

**Table 8. Kinetic Parameters of Coal Samples**

| code | temperature range/°C | apparent activation energy/kJ·mol$^{-1}$ | coefficient of determination $R^2$ | pre-exponential factor/min$^{-1}$ |
|---|---|---|---|---|
| HM | 304.3−446.8 | 90.7 | 0.9127 | 12.23 |
| HM-E | 306.9−449.5 | 120.7 | 0.9812 | $2.74 \times 10^3$ |
| HQL | 304.3−425.9 | 144.9 | 0.9706 | $4.28 \times 10^5$ |
| HQL-E | 307.0−477.0 | 148.4 | 0.9724 | $3.58 \times 10^5$ |

$$x = \frac{m_0 - m}{m_0} = \frac{\Delta m}{m_0} \times 100\% \quad (8)$$

In the formula, $x$ is the conversion of coal combustion reaction, %; $E$ is the apparent activation energy, kJ/mol; $A$ is the pre-exponential factor, $s^{-1}$; $m_0$ is the initial mass of the sample, g; $\Delta m$ is the weight loss of the sample at any time $t$, g; and $m$ is the mass of the sample at any time $t$ in the reaction, g; at the same time, setting temperature $T$ has a linear relationship with time $t$

$$T = T_0 + \lambda t \quad (9)$$

In this formula, $\lambda$ is the heating rate, constant, K/s.

The simultaneous 7 and 9 formulas can achieve the following approximate solutions

$$\ln\left[-\frac{\ln(1-x)}{T^2}\right] = \ln\left[\frac{AR}{\lambda E}\cdot\left(1 - \frac{2RT}{E}\right)\right] - \frac{E}{RT} \quad (10)$$

Because of the large value of $E$, the term $2RT/E$ can be approximately equal to zero. The linear fitting of $\ln[-\ln(1-x)/T^2] \sim 1/T$ can obtain a straight line. Its slope and intercept can calculate apparent activation energy $E$ and pre-exponential factor $A$, respectively. The calculation results are shown in Table 8.

After adding metal chelating agents, the apparent activation energy of HM coal sample increased by 33.08% and that of the HQL coal sample increased by 2.42%. It can be seen that EDTA can effectively complex metal ions in coal to reduce or lose catalytic activity and thus inhibit spontaneous combustion of coal. The inhibitory effect on different coal samples is different, which is related to the type and content of intrinsic metals in coal.

## 4. CONCLUSIONS AND FUTURE WORK

(1) Demineralization can remove most of the metals except aluminum in low-rank coal but has little effect on volatile matter, and the change of microcrystalline structure is not significant. The effect of demineralization on the coal structure mainly includes two parts: one is the removal of inorganic minerals, includes water-soluble salts and soluble minerals such as carbonates; the other is the removal of metals with an organically bound state, which are not closely bound with oxygen-containing functional groups, causing organic salts to become organic acids. The removed metal elements are mainly alkali metals Na and K, alkaline earth metals Ca, Mg, Sr, and Ba and transition metal Fe, Mn, Ti, and so forth. The main components that are not removed are mainly insoluble salts such as silicates and aluminosilicates.



https://doi.org/10.1021/acsomega.2c07741
ACS Omega 2023, 8, 13680−13689

(2) The temperature of weightlessness end point, ignition point, and maximum weightlessness rate point of the TG curve of demineralized coal increased. The heat absorbed by evaporation of water in coal and the heat released by oxidation and combustion of coal are decreased to different degrees, which indicates that the tendency of spontaneous combustion of de-ash coal is reduced from the perspective of heat change, indicating that the metal in coal plays a catalytic role in spontaneous combustion of coal.

(3) After adding the metal chelating agent EDTA, the apparent activation energy decreased by 33.08% and 2.42%, respectively. EDTA and the alkali metal, alkaline earth metal, or transition-metal ions formed a stable chelate in coal. The catalytic activity of metals is weakened or even lost, thereby inhibiting spontaneous combustion of coal, and verifying the catalytic effect of internal metals in coal on spontaneous combustion of coal.

The role of a certain metal element in coal is to study the basis of metal affecting spontaneous combustion of coal. The next step is to quantitatively analyze the catalytic effects of these elements on coal spontaneous combustion and further consider the effect of the interaction between various catalytic elements that actually exist on coal spontaneous combustion.

## AUTHOR INFORMATION


### Corresponding Author

**Yansheng Wang** − *College of Safety and Emergency Management Engineering, Taiyuan University of Technology, Taiyuan, Shanxi 030024, China;* orcid.org/0000-0001-5934-4287; Email: wangyansheng@tyut.edu.cn

### Authors

**Ling Qiao** − *College of Safety and Emergency Management Engineering, Taiyuan University of Technology, Taiyuan, Shanxi 030024, China*

**Xiaogang Mu** − *College of Safety and Emergency Management Engineering, Taiyuan University of Technology, Taiyuan, Shanxi 030024, China*

**Cunbao Deng** − *College of Safety and Emergency Management Engineering, Taiyuan University of Technology, Taiyuan, Shanxi 030024, China*

**Xuefeng Wang** − *College of Safety and Emergency Management Engineering, Taiyuan University of Technology, Taiyuan, Shanxi 030024, China*

Complete contact information is available at: https://pubs.acs.org/10.1021/acsomega.2c07741


### Author Contributions

L.Q.: experiment operation, writing—review & editing, writing—original draft, and funding acquisition. X.M.: experiment preparation and operation, C.D.: guidance for the project, X.W.: visualization and formal analysis, and Y.W.: conceptualization and methodology.

### Notes

The authors declare no competing financial interest.

## ACKNOWLEDGMENTS

The authors greatly acknowledge the financial support by Fundamental Research Program of Shanxi Province (202203021212295) and School Fund of Taiyuan University of Technology (2022QN134).

## REFERENCES


(1) Stracher, G. B.; Taylor, T. P. Coal fires burning out of control around the world: Thermodynamic recipe for environmental catastrophe. *Int. J. Coal Geol.* **2004**, *59*, 7−17.

(2) Rosema, A.; Guan, H.; Veld, H. Simulation of spontaneous combustion, to study the causes of coal fires in the Rujigou Basin. *Fuel* **2001**, *80*, 7−16.

(3) Smith, K. L.; Smoot, L. D.; Fletcher, T. H.; Pugmire, R. J. *The Structure and Reaction Processes of Coal*; Luss, D., Ed.; Plenum Press: New York, 1994; pp 1−419.

(4) Tang, X.; Huang, W. *Trace Elements in Chinese Coal*; The Commercial Press: Beijing, 2004.

(5) Kumar, S.; Wang, Z.; Zhang, K.; Xia, J.; Ronald, W.; He, Y.; Jaffri, G.-e.-R.; Bairq, Z. A.; Cen, K. F. Influence of temperature and $Ca(OH)_2$ on releasing tar and coal gas during lignite coal pyrolysis and char gasification. *Chin. J. Chem. Eng.* **2019**, *27*, 181−191.

(6) Liu, L. L.; Kumar, S.; Wang, Z. H.; He, Y.; Liu, J. Z.; Cen, K. F. Catalytic effect of metal chlorides on coal pyrolysis and gasification part I: combined TG-FTIR study for coal pyrolysis. *Thermochim. Acta* **2017**, *655*, 331−336.

(7) Zhang, F.; Xu, D.; Wang, Y. G.; Argyle, M. D.; Fan, M. H. $CO_2$ gasification of Powder River Basin coal catalyzed by a cost-effective and environmentally friendly iron catalyst. *Appl. Energy* **2015**, *145*, 295−305.

(8) Li, Y.; Yang, H. P.; Hu, J. H.; Wang, X. H.; Chen, H. P. Effect of catalysts on the reactivity and structure evolution of char in petroleum coke steam gasification. *Fuel* **2014**, *117*, 1174−1180.

(9) Zhou, L. M.; Zhang, G. J.; Reinmöller, M.; Meyer, B. Effect of inherent mineral matter on the co-pyrolysis of highly reactive brown coal and wheat straw. *Fuel* **2019**, *239*, 1194−1203.

(10) Liu, J. H.; Hu, H. Q.; Jin, L. J.; Wang, P. F.; Zhu, S. W. Integrated coal pyrolysis with $CO_2$ reforming of methane over Ni/MgO catalyst for improving tar yield. *Fuel Process. Technol.* **2010**, *91*, 419−423.

(11) Ma, X.; Zheng, G.; Sajjad, W.; Xu, W.; Fan, Q.; Zheng, J.; Xia, Y. Influence of minerals and iron on natural gases generation during pyrolysis of type-III kerogen. *Mar. Pet. Geol.* **2018**, *89*, 216−224.

(12) Mango, F. D.; Hightower, J. W.; James, A. T. Role of transition-metal catalysis in the formation of natural gas. *Nature* **1994**, *368*, 536−538.

(13) Medina, J. C.; Butala, S. J.; Bartholomew, C. H.; Lee, M. L. Iron-catalyzed $CO_2$ hydrogenation as a mechanism for coalbed gas formation. *Fuel* **2000**, *79*, 89−93.

(14) Xu, T.; Bhattacharya, S. Mineral Transformation and Morphological Change during Pyrolysis and Gasification of Victorian Brown Coals in an Entrained Flow Reactor. *Energy Fuels* **2019**, *33*, 6134−6147.

(15) Wu, Z.; Xu, L.; Wang, Z.; Zhang, Z. Catalytic effects on the ignition temperature of coal. *Fuel* **1998**, *77*, 891−893.

(16) Zou, C.; Wen, L.; Zhang, S.; Bai, C.; Yin, G. Evaluation of catalytic combustion of pulverized coal for use in pulverized coal injection (PCI) and its influence on properties of unburnt chars. *Fuel Process. Technol.* **2014**, *119*, 136−145.

(17) Gong, X.; Guo, Z.; Wang, Z. Reactivity of pulverized coals during combustion catalyzed by $CeO_2$ and $Fe_2O_3$. *Combust. Flame* **2010**, *157*, 351−356.

(18) Li, X. G.; Ma, B. G.; Xu, L.; Luo, Z. T.; Wang, K. Catalytic Effect of metallic oxides on combustion behavior of high ash coal. *Energy Fuels* **2007**, *21*, 2669−2672.

(19) Ma, B. G.; Li, X. G.; Xu, L.; Wang, K.; Wang, X. G. Investigation on catalyzed combustion of high ash coal by thermogravimetric analysis. *Thermochim. Acta* **2006**, *445*, 19−22.

(20) Gong, X.; Guo, Z.; Wang, Z. Variation on anthracite combustion efficiency with $CeO_2$ and $Fe_2O_3$ addition by Differential Thermal Analysis (DTA). *Energy* **2010**, *35*, 506−511.

(21) Wang, H.; Dlugogorski, B. Z.; Kennedy, E. M. Coal oxidation at low temperatures: Oxygen consumption, oxidation products, reaction mechanism and kinetic modelling. *Prog. Energy Combust. Sci.* **2003**, *29*, 487−513.
(22) Zhu, Q.; Jones, J.; Williams, A.; Thomas, K. The predictions of coal/char combustion rate using an artificial neural network approach. *Fuel* **1999**, *78*, 1755−1762.
(23) Tang, Y. The influences of manganese and phosphorus on the low-temperature oxidation of coal. *Int. J. Coal Prep. Util.* **2015**, *35*, 63−75.
(24) Larionov, K. B.; Mishakov, I. V.; Gromov, A. A.; Zenkov, A. V.; Strizhak, P. A.; Kuznetsov, G. V.; Zhdanova, A. O. Influence of $NaNO_3$ and $CuSO_4$ catalytic additives on coal oxidation process kinetic dependencies. *MATEC Web Conf.* **2017**, *91*, 01007.
(25) Zhang, D. K.; Sujanti, W. The effect of exchangeable cations on low-temperature oxidation and self-heating of a Victorian brown coal. *Fuel* **1999**, *78*, 1217−1224.
(26) Lv, H. P.; Li, B.; Deng, J.; Ye, L. L.; Gao, W.; Shu, C. M.; Bi, M. S. A novel methodology for evaluating the inhibitory effect of chloride salts on the ignition risk of coal spontaneous combustion. *Energy* **2021**, *231*, 121093.
(27) Qiao, L.; Deng, C.; Lu, B.; Wang, Y.; Wang, X.; Deng, H.; Zhang, X. Study on calcium catalyzes coal spontaneous combustion. *Fuel* **2022**, *307*, 121884.
(28) Lu, B.; Qiao, L.; Wang, J.; Zhang, J.; Ding, J. Experimental Study on the Influence of Pyrite Oxidation Products on Coal Spontaneous Combustion. *Int. J. Coal Prep. Util.* **2022**, *42*, 2581−2596.
(29) Liu, Y.; Zhao, W. B.; Zhang, Y. S.; Wang, J. F.; He, M.; Yang, M.; Hou, X. Influence of High Sulfate Mine Water on Spontaneous Combustion of Coal. *ACS Omega* **2022**, *7*, 46347−46357.
(30) Senior, C. L.; Zeng, T.; Che, J.; Ames, M. R.; Sarofim, A. F.; Olmez, I.; Huggins, F. E.; Shah, N.; Huffman, G. P.; Kolker, A.; Mroczkowski, S.; Palmer, C.; Finkelman, R. Distribution of trace elements in selected pulverized coals as a function of particle size and density. *Fuel Process. Technol.* **2000**, *63*, 215−241.
(31) Benson, S. A.; Holm, P. L. Comparison of inorganics in three low-rank coals. *Ind. Eng. Chem. Prod. Res. Dev.* **1985**, *24*, 145−149.
(32) Alvarez, R.; Clemente, C.; Gomez-limon, D. The influence of nitric acid oxidation of low rank coal and its impact on coal structure. *Fuel* **2003**, *82*, 2007−2015.
(33) Vasilakos, N. P.; Clinton, C. S. Chemical beneficiation of coal with aqueous hydrogen peroxide/sulphuric acid solutions. *Fuel* **1984**, *63*, 1561−1563.
(34) Liang, H.-Z.; Wang, C.-G.; Zeng, F.-G.; Li, M.-F.; Xiang, J.-H. Effect of demineralization on lignite structure from Yinmin coalfield by FT-IR investigation. *J. Fuel Chem. Technol.* **2014**, *42*, 129−137.
(35) Rubiera, F.; Arenillas, A.; Arias, B.; Pis, J. J.; Suarez-Ruiz, I.; Steel, K. M.; Patrick, J. W. Combustion behaviour of ultra clean coal obtained by chemical demineralisation. *Fuel* **2003**, *82*, 2145−2151.
(36) Song, Y.; Feng, W.; Li, N.; Li, Y.; Zhi, K. D.; Teng, Y. Y.; He, R. X.; Zhou, H. C.; Liu, Q. S. Effects of demineralization on the structure and combustion properties of Shengli lignite. *Fuel* **2016**, *183*, 659−667.
(37) Kizgut, S.; Baris, K.; Yilmaz, S. Effect of chemical demineralization on thermal behavior of bituminous coals. *J. Therm. Anal. Calorim.* **2006**, *86*, 483−488.
(38) Rubiera, F.; Arenillas, A.; Pevida, C.; Garcia, R.; Pis, J. J.; Steel, K. .M.; Patrick, J. W. Coal structure and reactivity changes induced by chemical demineralisation. *Fuel Process. Technol.* **2002**, *79*, 273−279.
(39) Kou, J. W.; Bai, Z. Q.; Bai, J.; Guo, Z. X.; Li, W. Effects of mineral matter and temperatures on conversion of carboxylic acids and their derivatives during pyrolysis of brown coals. *Fuel Process. Technol.* **2016**, *152*, 46−55.
(40) Liu, Q.; Hu, H. Q.; Zhou, Q.; Zhu, S. W.; Chen, G. H. Effect of inorganic matter on reactivity and kinetics of coal pyrolysis. *Fuel* **2004**, *83*, 713−718.
(41) Frazer, F. W.; Belcher, C. B. Quantitative determination of the mineral-matter content of coal by a radio frequency -oxidation technique. *Fuel* **1973**, *52*, 41−46.
(42) Zhou, C.; Liu, Q.; Li, Y. Production of hydrogen-rich syngas by steam gasification of Shengli liginite and catalytic effect of inherent minerals. *CIESC J.* **2013**, *64*, 2092−2102.
(43) Ibarra, J.; Muñoz, E.; Moliner, R. FTIR study of the evolution of coal structure during the coalification process. *Org. Geochem.* **1996**, *24*, 725−735.
(44) Painter, P. C.; Snyder, R. W.; Starsinic, M.; Coleman, M. M.; Kuehn, D. W.; Davis, A. Concerning the application of FTIR to the study of coal: a critical assessment of band assignments and the application of spectral analysis programs. *Appl. Spectrosc.* **1981**, *35*, 475−485.
(45) Li, Y.; Wang, Z. H.; Huang, Z. Y.; Liu, J. Z.; Zhou, J. H.; Cen, K. F. Effect of pyrolysis temperature on lignite char properties and slurrying ability. *Fuel Process. Technol.* **2015**, *134*, 52−58.
(46) Kister, J.; Guiliano, M.; Mille, G.; Dou, H. Changes in the chemical structure of low rank coal after low temperature oxidation or demineralization by acid treatment: Analysis by FT-i.r. and u.v. fluorescence. *Fuel* **1988**, *67*, 1076−1082.
(47) Michaelian, K. H.; Friesen, W. I. Photoacoustic FTIR spectra of separated western canadian coal macerals: analysis of the CH stretching region by curve-fitting and deconvolution. *Fuel* **1990**, *69*, 1271−1275.
(48) Geng, W. H.; Nakajima, T.; Takanashi, H.; Ohki, A. Analysis of carboxyl group in coal and coal aromaticity by Fourier transform infrared (FT-IR) spectrometry. *Fuel* **2009**, *88*, 139−144.
(49) Machado, A. d. S.; Mexias, A. S.; Vilela, A. C. F.; Osorio, E. Study of coal, char and coke fines structures and their proportions in the off-gas blast furnace samples by X-ray diffraction. *Fuel* **2013**, *114*, 224−228.
(50) Sonibare, O. O.; Haeger, T.; Foley, S. F. Structural characterization of Nigerian coals by X-ray diffraction, Raman and FTIR spectroscopy. *Energy* **2010**, *35*, 5347−5353.
(51) Nishino, J. Adsorption of water vapor and carbon dioxide at carboxylic functional groups on the surface of coal. *Fuel* **2001**, *80*, 757−764.
(52) Charrière, D.; Behra, P. Water sorption on coals. *J. Colloid Interface Sci.* **2010**, *344*, 460−467.


https://doi.org/10.1021/acsomega.2c07741
*ACS Omega* 2023, 8, 13680−13689